Holey metal films make perfect endoscopes

J. Jung,[1,2] F. J. García-Vidal,[2,*] L. Martín-Moreno,[3] and J. B. Pendry[4]
[1]*Department of Physics and Nanotechnology, Aalborg University, Skjernvej 4A, DK-9220 Aalborg Øst, Denmark*
[2]*Departamento de Física Teórica de la Materia Condensada, Universidad Autónoma de Madrid, E-28049 Madrid, Spain*
[3]*Departamento de Física de la Materia Condensada and Instituto de Ciencia de Materiales de Aragón (ICMA), CSIC-Universidad de Zaragoza, E-50009 Zaragoza, Spain*
[4]*Condensed Matter Theory Group, The Blackett Laboratory, Imperial College, London SW7 2BW, United Kingdom*
(Received 23 December 2008; revised manuscript received 18 March 2009; published 23 April 2009)

Possible superlensing effects in holey metal films are theoretically analyzed using the multiple-scattering formalism. We show that within the effective-medium limit and at some resonant frequencies, holey perfect conductor films make perfect endoscopes, i.e., are capable of transforming an image from the input to the output surface of the film with subwavelength resolution. To corroborate our finding in a realistic structure, a full numerical calculation including diffraction and losses is presented for a one-dimensional perforated metal film in the terahertz regime.

DOI: 10.1103/PhysRevB.79.153407 PACS number(s): 42.30.Wb, 41.20.Jb, 78.20.Ci

The idea of subwavelength imaging using a slab of an artificially engineered metamaterial (superlensing) was proposed some years ago.[1] It was proved that a thin slab of material with a refractive index of −1 yields a lens with almost unlimited resolution. The challenge is now to engineer a metamaterial with the desired optical properties. In the electrostatic limit, near-field superlensing can be obtained with a thin metal slab.[1–3] Examples of metamaterials that have been recently investigated for subwavelength imaging are layered metal-dielectric structures,[4–9] metallic wire media,[10–13] and electromagnetic (EM) or photonic crystals.[14–17]

The key to perfect lensing appearing in a homogeneous metal slab is the amplification of evanescent waves by means of resonantly excited surface plasmon polaritons (SPPs). More specifically, this phenomenon is linked to the existence of a flat region in the dispersion relation of SPPs for large parallel momenta at optical frequencies.[1] In this Brief Report we analyze whether this superlensing effect can be extended to lower frequencies by taking advantage of the so-called *spoof* SPPs.[18,19] These surface EM modes emerge when a perfect conductor film is perforated with a periodic array of apertures (see Fig. 1) and have similar characteristics to canonical SPPs. Here we will demonstrate that, contrary to the aforementioned expectations, superlensing effects do not appear in holey metal films. Instead, these structures can operate as perfect endoscopes, i.e., transmit all incident plane waves (propagating and evanescent) with unit efficiency at some resonant wavelengths.

Holey metal films have been extensively studied in recent years mainly in connection with the emergence of the phenomenon of extraordinary optical transmission.[20] In our theoretical analysis we first assume that all metal regions behave as perfect conductors, which is a good approximation in a wide range of frequencies, from dc up to terahertz frequencies. The effect of the finite absorption present in a real metal will be checked at a second stage.

An incident plane wave will excite several waveguide modes (TE and TM) within the holes but, in the very subwavelength regime, the fundamental mode dominates the transmission process because all higher-order modes are strongly evanescent. It is therefore a very good approximation in that limit to consider only the fundamental waveguide mode.[21] We also assume that the two surrounding dielectric media (1 and 3 in Fig. 1) and the medium within the apertures are the same. Within the single-mode approximation, the transmission coefficient of a holey metal film associated with the nth diffraction order can be written as a sum of all the multiple-scattering events,

$$t^{(n)} = \tau_{12}\tau_{23}^{(n)} \exp(iq_z h) + \tau_{12}\tau_{23}^{(n)}\rho^2 \exp(3iq_z h) + \tau_{12}\tau_{23}^{(n)}\rho^4 \exp(5iq_z h) + \cdots = \frac{\tau_{12}\tau_{23}^{(n)} \exp(iq_z h)}{1-\rho^2 \exp(2iq_z h)}, \tag{1}$$

where τ_{12}, $\tau_{23}^{(n)}$, and ρ are the different two-media scattering coefficients for a single interface and q_z is the propagation constant of the fundamental waveguide mode. τ_{12} is the transmission amplitude by which an incident plane wave in medium 1 is transmitted into medium 2, ρ is the reflection amplitude of the waveguide mode when it scatters from either interface 2-1 or 2-3, and $\tau_{23}^{(n)}$ is the transmission ampli-

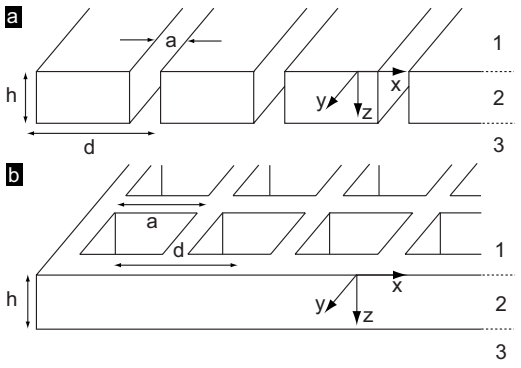

FIG. 1. Two examples of holey metal films. (a) One-dimensional metal film periodically perforated with subwavelength slits of width a and lattice constant d. (b) Two-dimensional metal film perforated with $a \times a$ square holes in a $d \times d$ lattice. The thickness of both films is h and extents along the z axis.

tude by which the waveguide mode, traveling towards the interface 2-3, transmits into a plane wave of diffraction order n that propagates away from the interface in medium 3. To simplify the notation, index n should be regarded as an index that comprises both polarizations and diffraction orders. The different two-media scattering coefficients can be determined by a proper matching of the parallel components of the EM field at the interfaces. After matching and substituting into Eq. (1) we obtain for $t^{(n)}$,

$$t^{(n)} = \frac{4Y_{\text{hole}}Y_0 S^{(0)*}S^{(n)} \exp(iq_z h)}{[Y_{\text{hole}}+G]^2 - [Y_{\text{hole}}-G]^2 \exp(2iq_z h)}, \tag{2}$$

where Y_{hole} is the admittance of the waveguide mode within the holes ($Y_{\text{hole}}=q_z/k_0$ if the fundamental mode is TE or $Y_{\text{hole}}=k_0/q_z$ for a TM mode) and $S^{(n)}$ is the overlap integral between an nth diffraction order and the fundamental waveguide mode. The term G contains a sum over diffracted modes, $G=\Sigma_{n=-\infty}^{\infty} Y_n |S^{(n)}|^2$, where Y_n is the admittance that relates the electric and the magnetic components of the plane waves in regions 1 and 3: $Y_n=k_0/k_z^{(n)}$ for p polarization and $Y_n=k_z^{(n)}/k_0$ for s polarization, with $k_z^{(n)}$ being the component of the wave vector along the z axis. The wave number in free space is $k_0=\omega/c$, where ω is the frequency and c the speed of light.

In the extreme subwavelength regime ($\lambda \gg d > a$), Eq. (2) can be further simplified if all diffraction effects are neglected. In this way, $t \equiv t^{(0)}$ becomes the only nonzero transmission coefficient,

$$t = \frac{4Y_{\text{hole}}Y_0 |S^{(0)}|^2 \exp(iq_z h)}{[Y_{\text{hole}}+Y_0|S^{(0)}|^2]^2 - [Y_{\text{hole}}-Y_0|S^{(0)}|^2]^2 \exp(2iq_z h)}. \tag{3}$$

Equation (3) is valid for both s and p polarizations, and the difference in the transmission enters via the admittances and the overlap integral $S^{(0)}$. In particular, for a p-polarized incident field, we obtain

$$t = \frac{4k_z q_z \varepsilon \exp(iq_z h)}{(q_z+\varepsilon k_z)^2 - (\varepsilon k_z - q_z)^2 \exp(2iq_z h)}, \tag{4}$$

where $k_z^{(0)}$ has been replaced with k_z and ε is given as

$$\varepsilon = \frac{q_z^2}{|S^{(0)}|^2 k_0^2}. \tag{5}$$

Equation (4) is exactly the transmission coefficient of p-polarized light through a homogeneous slab of thickness h characterized by a dielectric constant ε. Additionally, as the propagation constant inside the effective medium is q_z, the effective magnetic permeability is $\mu=|S^{(0)}|^2$. More precisely, in the two-dimensional (2D) case and for a square periodic array, the electric permittivity is a diagonal second-rank tensor with $\varepsilon_x=\varepsilon_y=\varepsilon$ and $\varepsilon_z=\infty$. In this case, $q_z=\sqrt{k_0^2-\pi^2/a^2}$ and $S^0=2\sqrt{2}a/(\pi d)$ and the permittivity shows a Drude-type behavior in which the cutoff frequency of the hole waveguide acts as an effective plasma frequency [see Eq. (5)]. The effective permeability takes a constant value $\mu_x=\mu_y=8a^2/(\pi^2 d^2)$. Interestingly, the same expressions for the electric permittivity and magnetic permeability were obtained when the concept of spoof SPP was first introduced,[18] although in that case the analysis was done for a semi-infinite slab, and not for a film of finite thickness. For the one-dimensional (1D) case, however, $\varepsilon_x=\varepsilon$ and $\varepsilon_y=\varepsilon_z=\infty$ with $q_z=k_0$ and $S^0=\sqrt{a/d}$. Thus, the 1D structure resembles an anisotropic dielectric medium with $\varepsilon_x=d/a$, $\mu_x=1$, and $\mu_y=\mu_z=a/d$.[19]

It is interesting to notice that Eq. (4) is equivalent to the expression that was used to demonstrate perfect lensing.[1] In the electrostatic limit, perfect lensing in an uncorrugated film is achieved when $\varepsilon \to -1$ because then $q_z=k_z$ for all parallel momenta $k_\parallel=\sqrt{k_x^2+k_y^2}$. For this condition, Eq. (4) reduces to $t=\exp(-ik_z h)$ for all $k_\parallel$, which shows how evanescent waves are amplified. For a holey metal film, however, q_z is fixed by the fundamental waveguide mode and it is not equal to $k_z=\sqrt{k_0^2-k_\parallel^2}$. Thus, we conclude that perfect lensing with holey metal films [requiring $t=\exp(-ik_z h)$ for all $k_\parallel$] cannot be realized. However, one may realize that at the Fabry-Pérot resonance condition ($q_z h = m\pi, m \geq 0$), Eq. (4) simplifies significantly to

$$t = e^{im\pi} = (-1)^m \; \forall \; k_\parallel. \tag{6}$$

At the Fabry-Pérot resonance condition, all incident plane waves (both propagating and evanescent) are perfectly transmitted through a holey perfect conductor film. This resonant regime where all incoming plane waves are transmitted with unit efficiency has been recognized before for metallic wire media.[10–13] Notice that the condition for excitation of spoof SPPs at large parallel momenta reads $q_z=0$, which fulfills the Fabry-Pérot resonance condition for $m=0$. Therefore, within the effective-medium limit ($\lambda \gg d > a$) and at the Fabry-Pérot resonances, Eq. (4) predicts that a holey perfect conductor film makes a perfect endoscope capable of transforming an image at the input surface with subwavelength resolution to the output surface of the film. This is the main conclusion of this Brief Report.

For proof-of-principle purposes, here in this Brief Report we analyze the simplest holey metal film: an infinite slit array [Fig. 1(a)]. The Fabry-Pérot resonance condition in this case is $\lambda=2h/m$ with $m \geq 1$. Given the input surface being at a distance z_1 from the incident field, we calculate the image at a distance z_2 from the output surface. The incident field is p polarized with its electric field directed along the x axis and consists of two spikes of height E_0, width w, and separation l. This field is expanded in terms of p-polarized plane waves characterized by parallel momentum $k_x^{(0)}$. From the knowledge of the different transmission coefficients $t^{(n)}$ [Eq. (2)] and by taking into account diffraction effects, it is straightforward to calculate the electric field at the image plane.

In order to approach the effective-medium limit where Eq. (4) is valid and where diffraction can be safely neglected, $t^{(0)} \gg t^{(n)}$ for $n \neq 0$ should be satisfied. For a slit array, $k_x^{(n)}=k_x^{(0)}+n\frac{2\pi}{d}$ and $k_z^{(n)}=i\sqrt{k_x^{(n)2}-k_0^2}$. If we choose parameters such that $\lambda \gg w \gg d$, it is obvious that the evanescent decay of all the diffracted waves for $n \neq 0$ is dominated by the term π/d, whereas the dominant $k_x^{(0)}$'s are on the order of π/w. Hence, in the extreme near field of the output surface (z_2

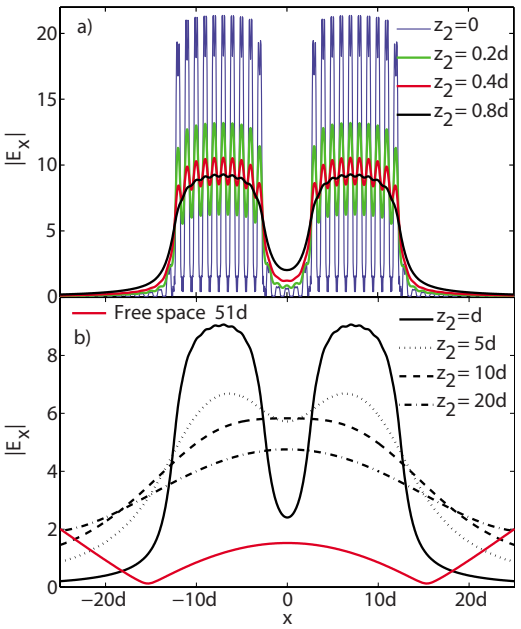

FIG. 2. (Color online) $|E_x(x)|$ for different distances z_2. The distance z_1 is chosen to be 0. d is used as the unit length of the structure and the resonant wavelength is $\lambda=2h=100d$. The width of the slits is $a=0.5d$ and the thickness of the film is $h=50d$. The parameters of the incident field are $E_0=10$, $l=15d$, and $w=10d$. In panel (b), it is also shown the image of the E field after free-space propagation through a $h+d$ distance (the curve with label free space $51d$).

≈ 0), higher-order diffracted waves will distort the perfect image that only can be obtained if diffraction can be completely neglected. However, one may realize that the higher-order diffracted waves will die much faster than the zero-order diffracted waves as $w \gg d$. Thus, if the distance from the output surface to the image plane z_2 is increased, the higher-order diffracted waves will disappear from the image. To illustrate this, we have calculated the image for different distances z_2 from the slit array [Fig. 2]. For details of the slit array, incident field, and wavelength, see caption of Fig. 2. It is clear that there are two near-field zones: one for $z_2 \ll d$, where the higher-order diffracted modes from the array distort the image [Fig. 2(a)] and the other one emerges at $d < z_2 < w$ where the image of the two spikes is recovered [Fig. 2(b)] with subwavelength resolution. Notice how the field for $z_2=d$ is nicely reconstructed in a subwavelength image of the source. In the absence of the holey metal film, most information of the source would be lost at this plane after free-space propagation [see the curve with label free space $51d$ in Fig. 2(b)]. This is also the case if the image plane is located at $z_2 \gg d$. As seen in Fig. 2(b), for $z_2 = 10d, 20d$ it is no longer possible to distinguish the two spikes of the incident field.

By reducing the width of the spikes and its separation (results not shown here), we have found that the ultimate resolution of the endoscope is d, which is the period of the array. This is similar to what occurs in the perfect lens in the optical regime,[1] in which the ultimate resolution would be the interatomic distance if the absorption in the metal film could be ignored.[22] We have also checked that almost identical images are obtained for film thicknesses $h_m = m\lambda/2$ ($m \geq 1$) that fulfill the Fabry-Pérot resonance condition at that particular wavelength. In this way, the thickness of the endoscope could be much larger than the operating wavelength.

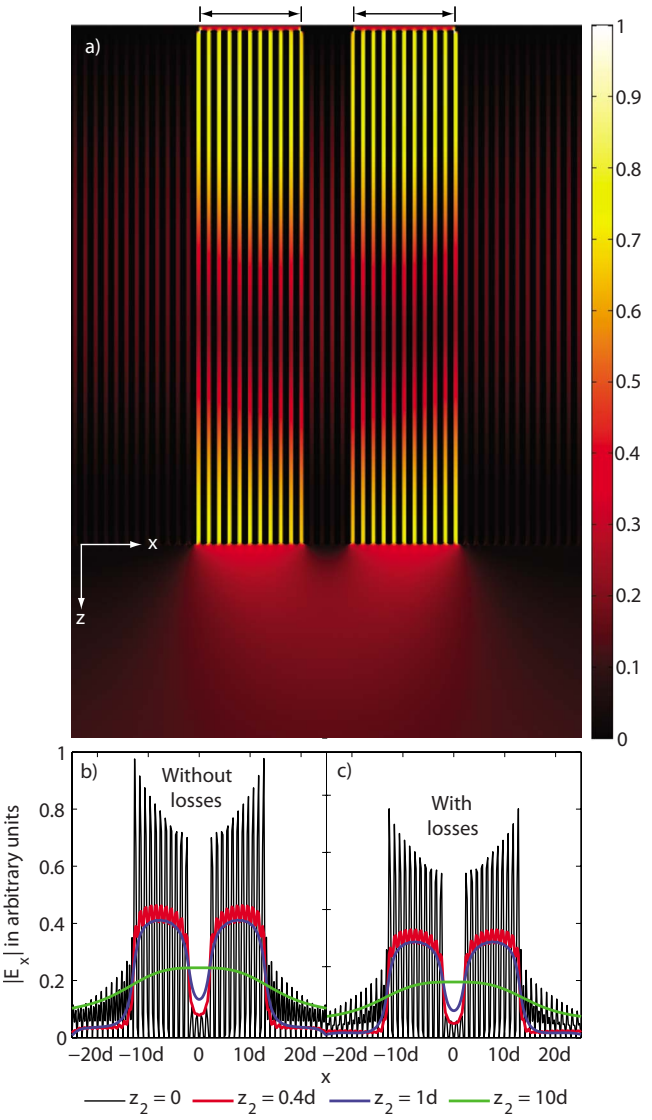

FIG. 3. (Color online) (a) E-field amplitude ($|E_x(x,z)|$) evaluated at the first Fabry-Pérot resonance. The incoming p-polarized field is impinging from above into an opaque screen in which two subwavelength apertures have been perforated (marked with arrows in the figure). The opaque screen is placed just in front of the input surface of the structure. The output surface of the slit array is marked by the x axis in the figure. (b) Calculation of $|E_x(x)|$ at different distances z_2 from the slit array in which Ohmic losses in the metal have not been included. (c) $|E_x(x)|$ at several z_2's that correspond to different cuts in the figure of panel (a).

To test the effect of the absorption in the metal and the accuracy of the single-mode approximation, we have carried out numerical calculations using the commercial finite element solver provided by COMSOL MULTIPHYSICS [Fig. 3]. We have considered a 1D slit array where the period is $d=1$ μm and the relation to all the other parameters of the film and source are the same as before (see caption of Fig. 2). This yields the first Fabry-Pérot resonance frequency at ν_0

=3 THz. Losses of the metal regions are included through the Drude model $\varepsilon_m = 1 - \omega_p^2/[\omega(\omega + i\Gamma)]$, where $\omega_p = 13.8 \times 10^{15}$ s^{-1} is the plasma frequency, $\Gamma = 1.075 \times 10^{14}$ s^{-1} is the damping constant, and the values are for gold and taken from Ref. 23. The 2D field distribution of $|E_x(x,z)|$ including losses is presented [Fig. 3(a)] and the image of the source for different distances z_2 is shown for both the cases without and with absorption [Figs. 3(b) and 3(c), respectively]. It is seen that the endoscope effect in holey metal films is not very sensitive to losses; the only difference when losses are included is a small damping of the field when compared to the lossless case.

In conclusion, we have shown how holey metal films can behave as perfect endoscopes at some resonant frequencies, i.e., they transmit light with unity efficiency for both propagating and evanescent incoming plane waves. In the terahertz regime, we have exemplified our ideas by means of a full numerical calculation on a 1D slit array where both diffraction effects and losses were included. Our findings suggest that holey metal films may find useful applications for subwavelength imaging.

We acknowledge Alexandre Mary for valuable discussions and financial support from the Spanish Ministry of Science under Project No. CSD2007-046-NanoLight.es and from a NABIIT project supported by the Danish Research Agency (Contract No. 2106-05-033).

*fj.garcia@uam.es

[1] J. B. Pendry, Phys. Rev. Lett. **85**, 3966 (2000).
[2] D. O. S. Melville and R. J. Blaikie, Opt. Express **13**, 2127 (2005).
[3] N. Fang, H. Lee, C. Sun, and X. Zhang, Science **308**, 534 (2005).
[4] S. A. Ramakrishna, J. B. Pendry, M. C. K. Wiltshire, and W. J. Stewart, J. Mod. Opt. **50**, 1419 (2003).
[5] P. A. Belov and Y. Hao, Phys. Rev. B **73**, 113110 (2006).
[6] B. Wood, J. B. Pendry, and D. P. Tsai, Phys. Rev. B **74**, 115116 (2006).
[7] Y. Xiong, Z. Liu, and X. Zhang, Appl. Phys. Lett. **93**, 111116 (2008).
[8] Z. Liu, H. Lee, Y. Xiong, Ch. Sun, and X. Zhang, Science **315**, 1686 (2007).
[9] I. I. Smolyaninov, Y.-J. Hung, and C. C. Davis, Science **315**, 1699 (2007).
[10] P. A. Belov, Y. Hao, and S. Sudhakaran, Phys. Rev. B **73**, 033108 (2006).
[11] G. Shvets, S. Trendafilov, J. B. Pendry, and A. Sarychev, Phys. Rev. Lett. **99**, 053903 (2007).
[12] S. Kawata, A. Ono, and P. Verma, Nat. Photonics **2**, 438 (2008).
[13] P. A. Belov, Y. Zhao, S. Tse, P. Ikonen, M. G. Silveirinha, C. R. Simovski, S. Tretyakov, Y. Hao, and C. Parini, Phys. Rev. B **77**, 193108 (2008).
[14] P. A. Belov, C. R. Simovski, and P. Ikonen, Phys. Rev. B **71**, 193105 (2005).
[15] P. Ikonen, P. Belov, C. Simovski, and S. Maslovski, Phys. Rev. B **73**, 073102 (2006).
[16] C. Luo, S. G. Johnson, J. D. Joannopoulos, and J. B. Pendry, Phys. Rev. B **65**, 201104(R) (2002).
[17] P. V. Parimi, W. T. Lu, P. Vodo, and S. Sridhar, Nature (London) **426**, 404 (2003).
[18] J. B. Pendry, L. Martin-Moreno, and F. J. Garcia-Vidal, Science **305**, 847 (2004).
[19] F. J. Garcia-Vidal, L. Martin-Moreno, and J. B. Pendry, J. Opt. A, Pure Appl. Opt. **7**, S97 (2005).
[20] T. W. Ebbesen, H. J. Lezec, H. F. Ghaemi, T. Thio, and P. A. Wolff, Nature (London) **391**, 667 (1998).
[21] L. Martin-Moreno, F. J. Garcia-Vidal, H. J. Lezec, K. M. Pellerin, T. Thio, J. B. Pendry, and T. W. Ebbesen, Phys. Rev. Lett. **86**, 1114 (2001).
[22] F. D. M. Haldane, arXiv:cond-mat/0206420 (unpublished).
[23] L. Novotny and B. Hecht, *Principles of Nanooptics* (Cambridge University Press, Cambridge, England, 2006).